Measurements and Monte Carlo simulations of high-energy neutron streaming through the access maze using activation detectors at 24 GeV/c proton beam facility of CERN/CHARM

Noriaki Nakao, Tsuyoshi Kajimoto, Toshiya Sanami, Robert Froeschl, Elpida Iliopoulou, Angelo Infantino, Hiroshi Yashima, Takahiro Oyama, Seiji Nagaguro, Eunji Lee, Tetsuro Matsumoto, Akihiko Masuda, Yoshitomo Uwamino, Stefan Roesler & Markus Brugger

Taylor & Francis
Taylor & Francis Group

ARTICLE

Measurements and Monte Carlo simulations of high-energy neutron streaming through the access maze using activation detectors at 24 GeV/c proton beam facility of CERN/CHARM

Noriaki Nakao [a], Tsuyoshi Kajimoto[b], Toshiya Sanami [c], Robert Froeschl [d], Elpida Iliopoulou [d,e], Angelo Infantino [d], Hiroshi Yashima[f], Takahiro Oyama [c], Seiji Nagaguro[c], Eunji Lee [g,h], Tetsuro Matsumoto [i], Akihiko Masuda [i], Yoshitomo Uwamino [a], Stefan Roesler [d] and Markus Brugger [d]

aInstitute of Technology, Shimizu corporation, Tokyo, Japan; bHiroshima University, Hiroshima Japan; cHigh Energy Accelerator Research Organization (KEK), Ibaraki Japan; dCERN, Geneva Switzerland; eHirslanden Private Hospital Group, Radiation Oncology Institut, Lausanne Switzerland; fKyoto University (KURNS), Osaka Japan; gKyushu University, Fukuoka Japan; hDepartment of Nuclear Engineering, North Carolina State University, Raleigh, NC, USA; iNational Institute of Advanced Industrial Science and Technology (AIST), Ibaraki Japan

ABSTRACT

A measurement of high-energy neutron streaming was performed through a maze at the CERN (Conseil Européen pour la Recherche Nucléaire) High-energy AcceleRator Mixed-field (CHARM) facility. The protons of 24 GeV/c were injected onto a 50-cm-thick copper target and the released neutrons were streamed through a maze with several corridor-legs horizontally designed with the shield walls in the facility. Streaming neutrons were measured by using aluminum activation detectors placed at 10 locations in the maze. From the radionuclide production rate in the activation detectors, the attenuation profile along the maze was obtained for the reaction of $^{27}Al(n,\alpha)^{24}Na$. Monte Carlo simulations performed with two codes, the Particle and Heavy Ion Transport System (PHITS) and CERN FLUktuierende KAskade (FLUKA), gave good agreements with the measurements within a factor of 1.7 for the production rates ranging over more than 3 orders of magnitude.

Introduction

Particle accelerator facilities have been constructed for physics, medical and industrial uses. Accelerator specifications have been upgraded to enhance the intensity and energy of the particle beam to provide better statistics and more efficient irradiation. To ensure the radiation safety in these facilities, the prompt- and residual-radiation levels should be predicted from secondary neutrons generated by beam irradiation. Since the neutrons highly penetrate a shield and stream through a maze, facility structures with massive shields and bending mazes should be well designed to reduce the radiation outside the facility to acceptable and optimized levels. As the radiation shield occupies a considerable portion of the total construction costs and, cannot be easily modified once the facility is built, the facility design is very important when constructing high-intensity and high-energy accelerators.

Until now, a number of measurements of neutron streaming at mazes have been conducted, but, most of them have been for fission neutrons. For high energy neutrons above 20 MeV, experimental data of maze streaming are very scarce. A measurement of high-energy neutron streaming at a maze was conducted by Tanaka et al. [1] in the Takasaki Ion Accelerators for Advanced Radiation Application (TIARA) of the Japan Atomic Energy Research Institute (JAERI, currently QST(National Institutes for Quantum and Radiological Science and Technology)). In the experiment, neutrons were produced at a thick copper target bombarded by 68-MeV proton beam, and the neutron energy spectra along the maze were measured using an organic liquid scintillator and Bonner spheres. It was reported that dose equivalent distribution estimated from the experimental results agreed within a factor of three with that calculated by the empirical formulae. However, accuracy of Monte Carlo calculations was not confirmed with the experiment.

Recently, for safety purpose in the accelerator facility, a radiation transport simulation with Monte Carlo codes is the main method to predict the radiation levels in the various locations during and after beam operations. In order to know accuracy of the results with simulation codes, validation with experimental data is indispensable.

At the CERN High-energy AcceleRator Mixed-field (CHARM) facility [2,3], deep-penetration shielding experiments were performed in 2015 [4–7] by our experimental team. Using the same facility, an experiment of a maze streaming was performed in 2018. This paper reports the study of experimentally evaluated

high-energy neutron fluxes along a maze at the CHARM. The Monte Carlo simulations were also carried out and validated by comparisons between the experimental and simulated results.

Experiment

Facility

Figure 1 shows the horizontal structure of the CHARM facility in the east hall at CERN. 24-GeV/c protons are transported from the Proton Synchrotron (PS) and injected onto a copper target (8-cm diameter by 50-cm thickness) located at the center of the facility. The protons not interacting in the target are transported into an iron beam dump placed downstream. The proton beam line and target room are surrounded by concrete and iron shields. The target room can only be accessed through a maze structure which has a corridor with several legs.

Figure 2 shows the vertical shielding structure of the CHARM facility, which is perpendicular to the beam axis at the target location. The target center is positioned on the beam line which is 129 cm above the floor. To the right of the target in Figure 2, there is a four-layered movable shield wall of steel and concrete. Each of the shield layer is 20-cm thickness and 214-cm height from the floor. Above the ceiling of the target room, located 240 cm above the beam line, a bulk shield consists of 80-cm-thick cast iron and 360-cm-thick ordinary concrete. A 10-cm-thick marble ceiling is installed at 185 cm above the beam line (below the iron ceiling). Compositions and densities of the shield materials are listed in Table 1.

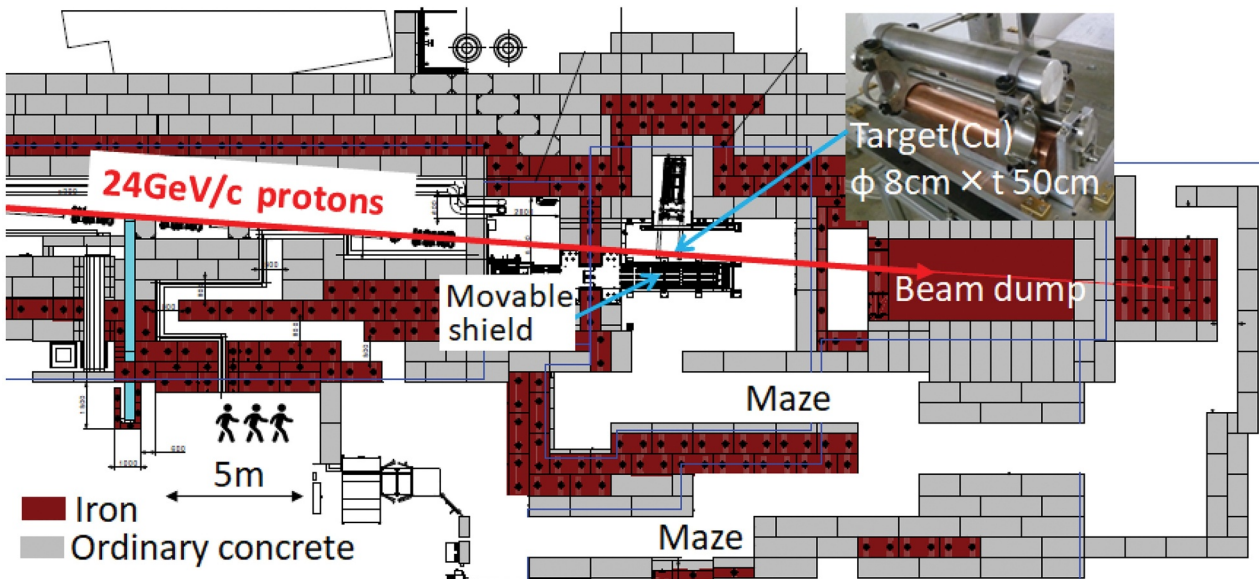**Figure 1.** Horizontal cross-section of the CHARM facility.
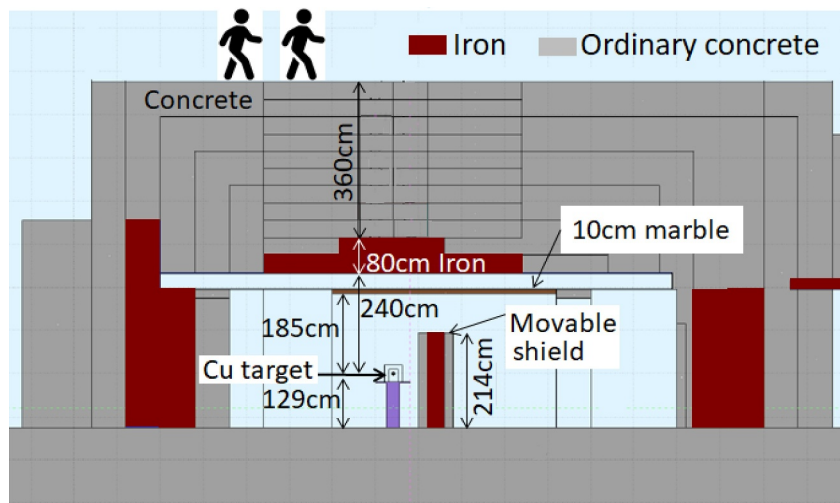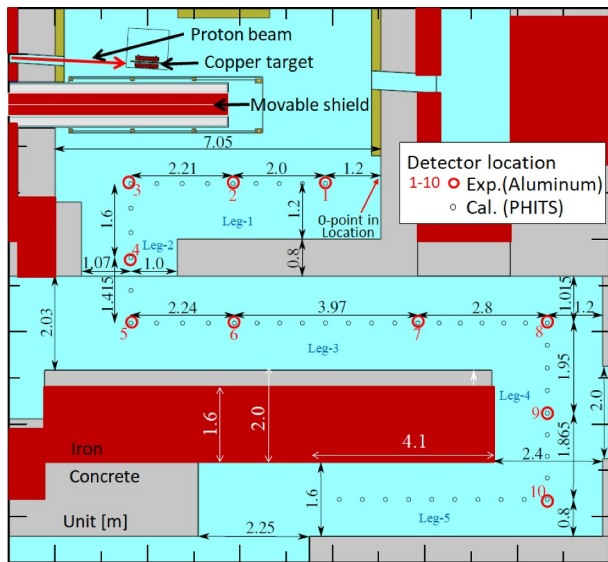

Figure 2. Vertical cross-section of the shield structure in the CHARM facility perpendicular to the beam axis at the target location. The beam travels from front to back of this figure.

Table 1. Density and chemical composition of the materials used in the present experiment.

Material	Element	Weight	Element	Weight
Density [g/cm³]		[%]		[%]
Concrete	H	0.561	Si	16.175
2.4	C	4.377	S	0.414
	O	48.204	K	0.833
	Na	0.446	Ca	23.929
	Mg	1.512	Ti	0.173
	Al	2.113	Fe	1.263
Cast Iron	Fe	92.3	P	0.08
7.2	C	3.85	S	0.02
	Mn	0.3	Co	0.05
	Si	3.4		
Movable Shield	Fe	97.793	P	0.035
(Steel S235JR)	C	0.17	S	0.035
7.85	Mn	1.4	N	0.012
	Cu	0.55	Co	0.005

Figure 4. Photos of activation detectors in the maze.

Figure 3. Maze structure and detector locations.

Activation detectors and experimental setup

The streaming neutrons through the maze were measured by activation detectors composed of aluminum (2.7 g/cm³, 99.99% purity), which is widely used in high-energy neutron measurements [8]. Two sizes of the aluminum (ϕ 8.0 cm × t 1.0 cm and ϕ 4.0 cm × t 0.4 cm, where ϕ is the diameter and t is the thickness) were used depending on the neutron intensity in the corresponding locations. As shown in Figure 3, the activation detectors were placed at 10 locations at the beam line height and the horizontal center of the corridors along the five legs of the maze. Photos of activation detector set-up are shown in Figure 4.
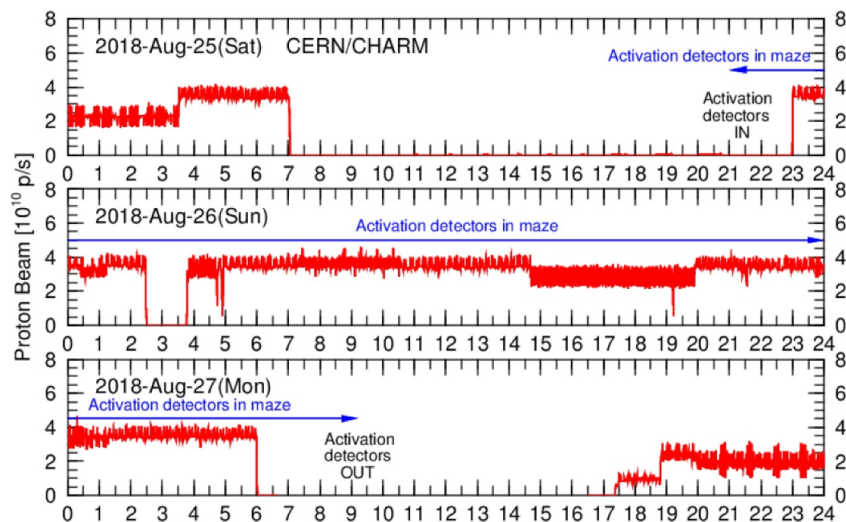
Figure 5. History of beam intensity during the irradiation (hours of the given days indicated).

Table 2. Production reaction, half-life, photon energies and emission ratios of the radionuclide in the aluminum activation detector.

Reaction	Half Life	Photon Energy	Emission Ratio
^{27}Al(n,α)^{24}Na	14.96 h	1368.6 keV	1.000
		2754.6 keV	0.999

Beam irradiation

The maximum average intensity of the 24-GeV/c proton beam at CHARM is 6.7×10^{10} proton/sec (p/s) [9]. The actual beam intensity is monitored by a Secondary Emission Chamber (SEC), which was calibrated using the aluminum activation method. Figure 5 shows the average-intensity history measured by the SEC during the experiment. The intensity ranged from 2×10^{10} to 4×10^{10} p/s. The beam irradiation was carried out for about 1 day and 7 hours in the weekend.

The activation detectors were removed after the irradiation and transported to a gamma-ray measurement station located in the east hall. Energy spectra of photons from radionuclides generated in the activation detectors by ^{27}Al(n,α)^{24}Na reaction were measured there by using a high-purity germanium-semiconductor (HPGe) detector. The measurements were conducted for time between 3 and 24 hours depending on the peak count rates of the photons from ^{24}Na.

Data analysis

Table 2 lists the analyzed radionuclide-production reaction, half-life, and photon energies with their emission ratios. The net counts of the photo-peak at the corresponding photon energies were analyzed, and the production rates of the radionuclides in the activation detectors per proton were estimated from the photo-peak efficiencies of the HPGe-detector and the beam-intensity during the irradiation shown in Figure 5. The analysis method is detailedly described in Ref [4]. The efficiencies of the HPGe-detector were estimated in LabSOCS software (Mirion Technologies Canberra KK) [10].

Monte Carlo Simulations

Simulation set up

A Monte Carlo simulation was performed with the Particle and Heavy Ion Transport code System (PHITS) Ver-3.20 [11]. Although Ver-3.02 is cited as the reference, there is no difference between the two versions in the compiled data for the transport simulation in this work. To simulate the reactions of neutrons above 20 MeV and protons, the evaporation model GEM [12], the intra-nuclear cascade model
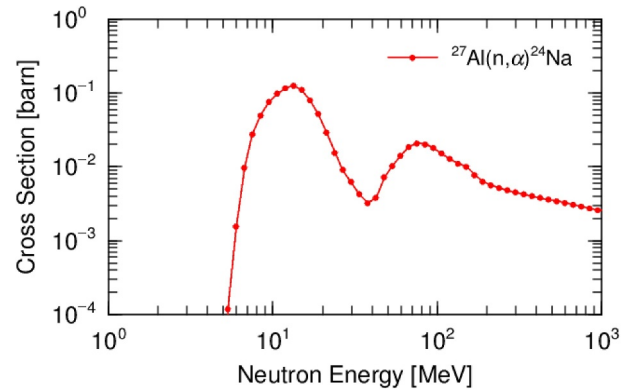
Figure 6. Cross-sections of activation reaction for aluminum.

INCL [13] up to 3 GeV, and the high-energy nuclear reaction model JAM [14] above 3 GeV were used in the PHITS code. For neutrons below 20 MeV, the JENDL-4.0 data library [15] was used.

Another Monte Carlo simulation was also performed with the CERN FLUKA code, Version 4.0.0, and a detailed description of the models and cross-section data used in FLUKA can be found in Ref [16,17].

### Simulation for maze streaming

Since the maze structure was complicated, the simulations with both the codes were performed with a full geometry as shown in Figures 1–3. For the PHITS simulation, the neutron energy spectra were obtained using track-length estimators of 10-cm diameter spheres. The spheres were set at 49 positions on the horizontal center of the maze at the beam-line height along the 5 legs, as shown in Figure 3. The locations of these spherical estimators included the corresponding 10 locations of the aluminum activation detectors in the experiment. For the FLUKA simulation, the neutron energy spectra were scored using track-length estimators (size of 20-cm×20-cm× 20-cm) at the 10 experimental locations. The whole shield structure shown in Figures 1 and Figures 2 were considered in the geometries for both PHITS and FLUKA, including 3.6-m-thick top-roof concrete, 2-m-thick floor concrete, the beam dump and side shields which are thick enough to consider scattering neutrons in the maze.

Calculated production rate

The radionuclide production rates were estimated by folding (multiplying and integrating) the simulated energy spectra with the cross-section of ^{27}Al(n, α)^{24}Na reaction. The cross-section data, plotted in Figure 6, were obtained from the Maekawa library [18], which was evaluated on the basis of the experimental data by Kim et al. [19].

Table 3. Numerical values for experimental and calculated radionuclide production rates, their uncertainties in percentage for 10 locations of activation detectors in the experiment.

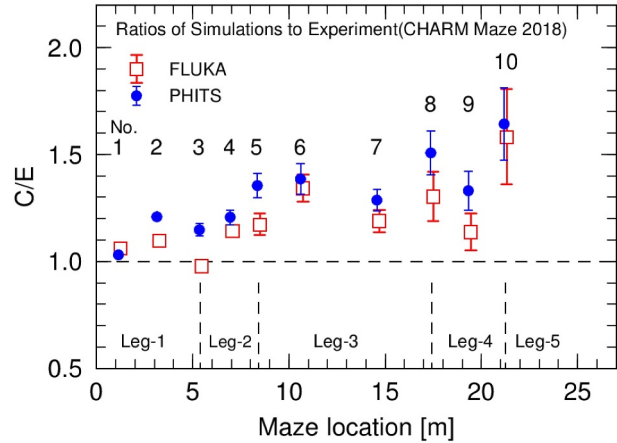| No.	Location	Experiment	Unc	PHITS	Unc	FLUKA	Unc
	[m]	[^{24}Na/atom/proton]	[%]	[^{24}Na/atom/proton]	[%]	[^{24}Na/atom/proton]	[%]
1	1.200	1.95×10^{-31}	1.78	2.01×10^{-31}	0.47	2.07×10^{-31}	0.40
2	3.200	1.25×10^{-31}	1.93	1.51×10^{-31}	0.54	1.37×10^{-31}	0.48
3	5.410	6.75×10^{-32}	2.46	7.75×10^{-32}	0.73	6.60×10^{-32}	0.71
4	7.010	4.08×10^{-32}	2.62	4.92×10^{-32}	0.93	4.66×10^{-32}	0.85
5	8.425	1.63×10^{-32}	4.07	2.21×10^{-32}	1.37	1.91×10^{-32}	1.26
6	10.665	3.65×10^{-33}	4.58	5.06×10^{-33}	2.67	4.90×10^{-33}	1.44
7	14.635	2.12×10^{-34}	3.93	2.73×10^{-34}	0.57	2.52×10^{-34}	1.88
8	17.435	2.90×10^{-34}	6.69	4.37×10^{-34}	1.51	3.78×10^{-34}	5.58
9	19.385	3.06×10^{-34}	6.67	4.07×10^{-34}	1.36	3.48×10^{-34}	3.62
10	21.250	4.50×10^{-35}	9.58	7.39×10^{-35}	3.65	7.12×10^{-35}	10.24
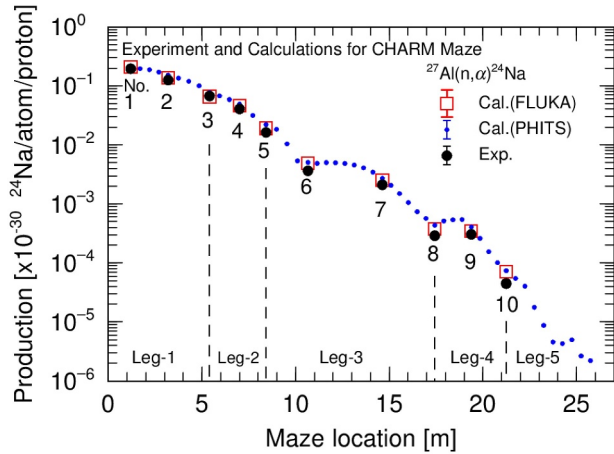
Figure 7. Attenuation profile of experimental production rates along the maze compared with the calculated ones.

Figure 8. Ratios of calculated to experimental production rates (C/E) of radionuclides at different locations along the maze.

Table 4. Summary of uncertainties.

	Source of uncertainty	Uncertainty on production rate
Experiment	γ-spectrometry statistics	1.78–9.58%
	γ-spectrometry efficiency	4.3%
	Activation detector weight	1%
	Beam monitor calibration	7%
	Beam intensity statistics	<1%
	Beam momentum	<1%
	Beam position and profile	<1%
	Target density and dimension	<1%
Simulation	Statistics (PHITS)	0.47–3.65%
	Statistics (FLUKA)	0.4–10.24%

Results and Discussion

Table 3 gives numerical values of the ^{24}Na production rates at the 10 locations of activation detectors in the experiment. Figure 7 shows the attenuation profile of the measured production rate through the maze. The location given with the unit of meter in Table 3 and Figure 7 is the distance from the surface of the downstream wall of the irradiation room as shown in Figure 3. It is observed that the ^{24}Na production rate decreases with the distance along the maze. The experimental uncertainties in the figures and the table are statistical uncertainties of the gamma-ray counting. The uncertainties in the HPGe-detector efficiency by the LabSOCS (4.3%) [10] and the beam-intensity-monitor

calibration (7%) [5] are not included. Table 4 summarizes all the uncertainties.

For comparison, production rates calculated with the PHITS and FLUKA codes are also tabulated in the Table 3 and plotted in Figure 7. The errors of the calculations in the figures and table are statistical errors of the Monte Carlo simulations. For the PHITS results, all production rates calculated at 49 locations are shown in Figure 7. Generally, the calculated results of both the PHITS and FLUKA codes agree with experimental results over the whole region along the maze. To investigate discrepancies between the measured and calculated production rates in detail, ratios of calculated to experimental production rates (C/E) are plotted in Figure 8. The C/E increases with the increase of the distance along the maze, and this discrepancy might be attributed to the Monte Carlo simulations or the applied reaction cross-sections. However, the calculated results generally agree with the experiment within 30% in Leg-1 and Leg-2 of the maze. On the other hand, the differences become larger in Leg-3 or further, and the discrepancy is 65%, i.e. a factor of ~1.7, in the worst case. The calculated results by PHITS and FLUKA generally give a good agreement with each other.

Around the experimental location No.9 in Leg-4, higher production rates than those around the location No.8 are observed in both the experiment and
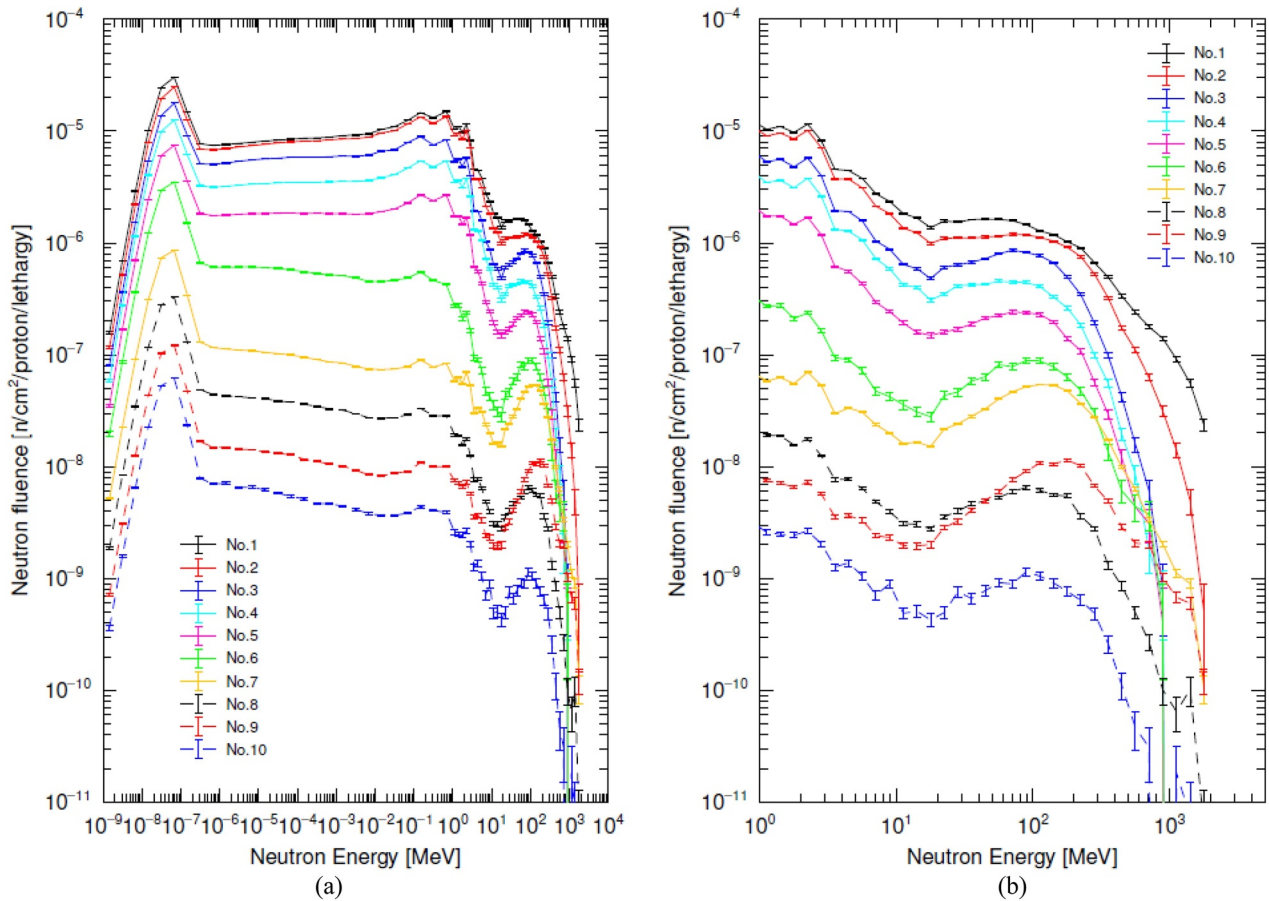
Figure 9. Neutron energy spectra simulated with PHITS code at 10 locations for (a) whole energy region and (b) region above 1 MeV.
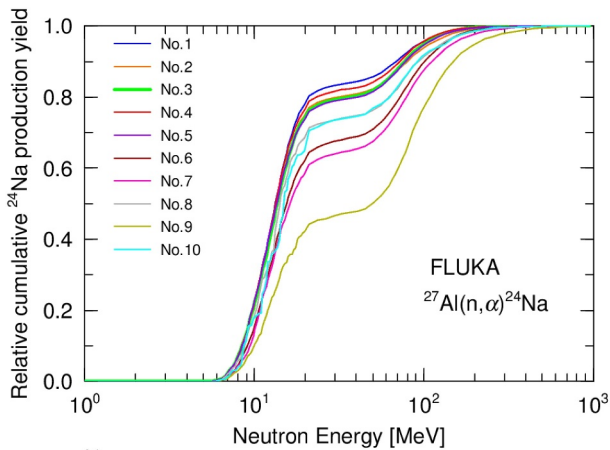
Figure 10. Relative cumulative ^{24}Na production yields as a function of neutron energy estimated with the neutron energy spectra simulated with FLUKA code for 10 locations.

simulation. It can be considered that this phenomenon was caused by a contribution of high-energy neutrons that penetrated the movable and the 80-cm-thick shield.

Figure 9 shows neutron energy spectra at the detector locations in the maze obtained from the PHITS simulation. It can be seen in Figure 9A that the energy spectra from thermal to maximum energy decrease with increasing the distance along the maze. Figure 9B shows neutron energy spectra focusing on the energy region above 1 MeV. The neutron spectra of No. 7 and 9 are higher than those of previous locations: No.6 and 8 in the energy region above 300 MeV and 40 MeV, respectively. At the locations of No.7 and 9, the neutrons passing through the shield wall are significantly added to those streaming along the maze as to be mentioned later.

Figure 10 shows the relative cumulative ^{24}Na production yields as a function of neutron energy estimated with the cross-section data and energy spectra simulated with FLUKA code for 10 locations. Relative contributions of the neutron energy regions to the ^{24}Na production can be found from the distribution, and it is indicated that neutrons of energy higher than 50 MeV greatly contribute to the productions at the position of No. 9.

Figure 11 shows two-dimensional distributions simulated for neutron flux above 1 MeV by PHITS and ^{24}Na production [20,21] by FLUKA in the horizontal plane. Since the threshold of the ^{27}Al(n,α)^{24}Na reaction is around a few MeV, distributions of neutrons in the energy range above a few MeV can be observed from both of the color plots, and a flow of neutrons through the wall between Leg-1 and Leg-3
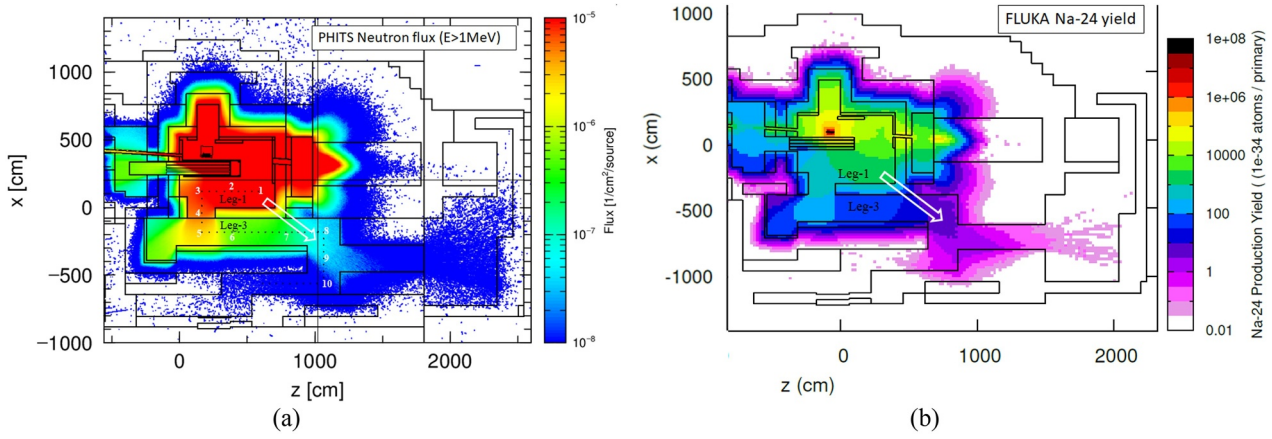
Figure 11. Two-dimensional flux distributions in the horizontal plane simulated for (a) neutron flux (E>1MeV) by PHITS and (b) ^{24}Na production yield by FLUKA.
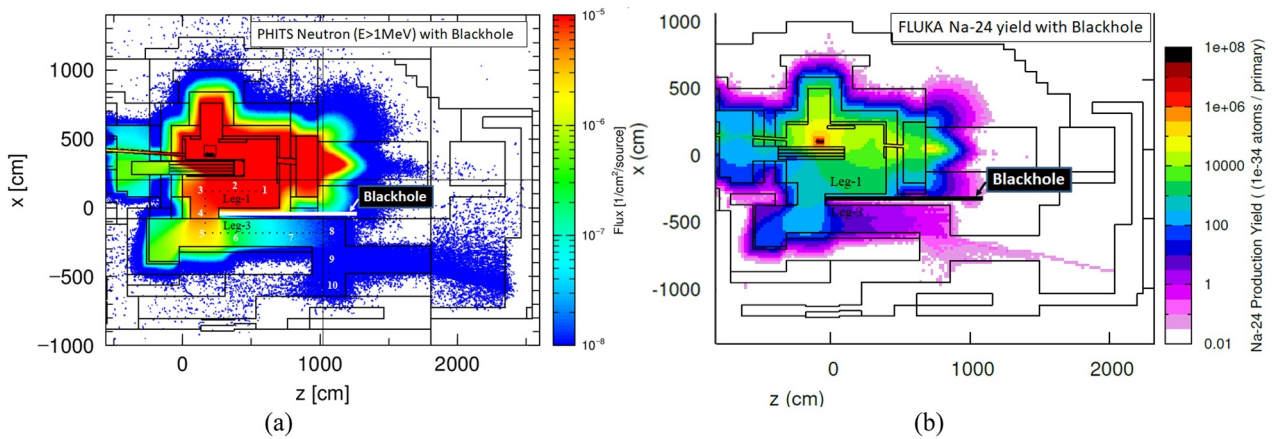

Figure 12. Two-dimensional flux distributions in the horizontal plane with a black-hole (solid line in the figure) inside the wall between Leg-1 and Leg-3 simulated for (a) neutron flux (E>1MeV) by PHITS and (b) ^{24}Na production yield by FLUKA.

can be seen as shown with the arrows. It is considered that the high-energy neutrons at the maze in this facility are composed of transmitted neutrons through bulk shield in addition to the streaming neutrons through the maze. In order to investigate the phenomenon, additional simulations by both PHITS and FLUKA were performed with additional zero importance region (black-hole), where any particle transport is terminated, inside the wall between Leg-1 and Leg-3. Height range of the black-hole is between the inner surfaces of the floor (129 cm below the beam axis) and the ceiling (195 cm above the beam axis). Figure 12 shows the two-dimensional distributions calculated with incorporating the black-hole. It can be seen that stopping of the neutron flow through the wall drastically reduces the neutron intensity in the legs after Leg-3.

Figure 13 shows neutron energy spectra simulated by PHITS and FLUKA in the locations of the activation detectors from No.5 to No.10 along Leg-3 and Leg-4 in the maze with and without the black-hole inside the wall. It can be found that the higher energy components above around 10 MeV for the

calculations with the black-hole were less than one tenth of those without black-hole. This indicates that penetration components through the wall between Leg-1 and Leg-3 are dominant in the higher energy region. Neutron energy spectra simulated by PHITS and FLUKA give good agreements with each other.

The attenuation profiles of ^{24}Na production rate along the maze are compared between with and without the black-hole in Figure 14. It can be seen that penetrating component is dominant beyond Leg-3, and the production rates due to the streaming neutrons are small by one order of magnitude to those due to the total neutrons. It is important to know the behavior of high-energy neutrons in the maze because the lower-energy neutrons decrease much faster and are produced mainly by the scattering of high-energy neutrons and also because the effective dose is typically dominated by high-energy neutrons.

Conclusion

A high-energy neutron streaming through the maze at the CHARM facility at CERN was measured using the
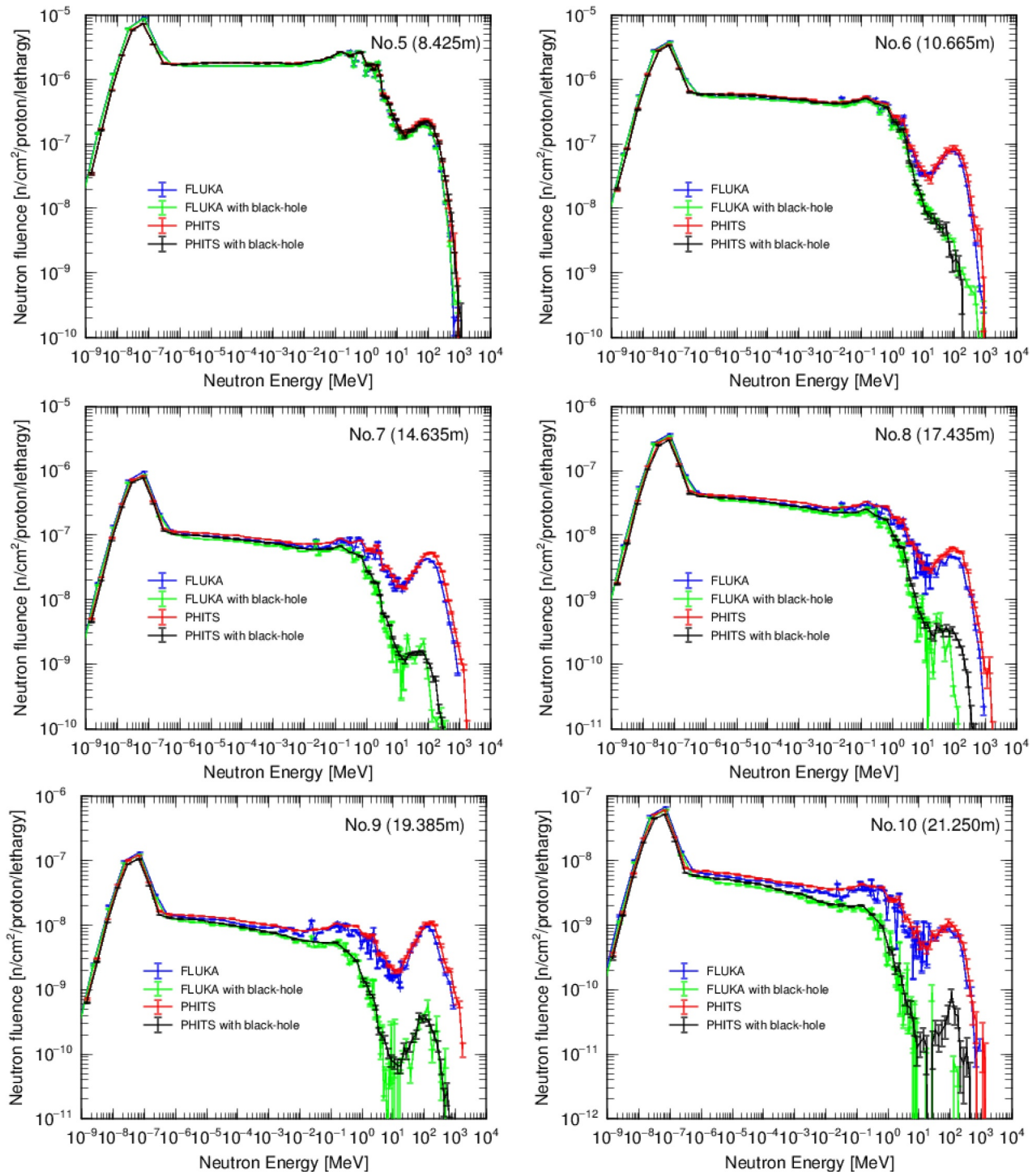
Figure 13. Neutron energy spectra simulated by PHITS and FLUKA in the locations of the activation detectors from No.5 to No.10, compared with those with the black-hole inside the wall.

^{27}Al(n,α)^{24}Na reaction. The source neutrons were generated at the 50-cm-thick copper target bombarded by 24 GeV/c protons. The results of Monte Carlo simulations performed with PHITS and FLUKA codes reasonably agreed with the measured data within a factor of 1.7. Due to the additional simulations, it was found that the penetration component of high-energy neutrons through the shield between the legs in the maze contributed significantly to the further locations of the maze. In the high-energy particle accelerator facility, it is

important to estimate the behavior of high-energy neutrons because most of low energy neutrons at the downstream of the maze are produced mainly by the scattering of high-energy neutrons from the upstream of the maze.

This work provides benchmark experimental data for a maze streaming in a high-energy proton accelerator facility. The results are expected to improve our understanding of shielding design in future high-energy accelerator facilities.
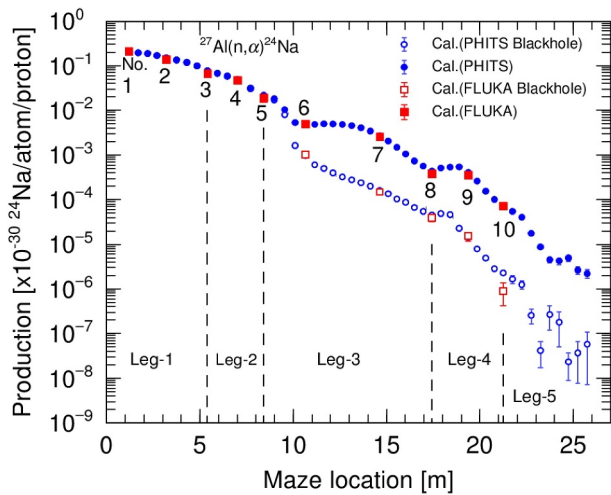
Figure 14. Attenuation profiles of production rates along the maze simulated by PHITS and FLUKA, and those with the black-hole inside the wall.

Acknowledgments

Disclosure statement

No potential conflict of interest was reported by the authors.

ORCID

Noriaki Nakao http://orcid.org/0000-0002-5910-8222
Toshiya Sanami http://orcid.org/0000-0003-2255-8008
Robert Froeschl http://orcid.org/0000-0002-2194-5869
Elpida Iliopoulou http://orcid.org/0000-0003-0895-9227
Angelo Infantino http://orcid.org/0000-0002-7854-3502
Takahiro Oyama http://orcid.org/0000-0002-9425-0275
Eunji Lee http://orcid.org/0000-0002-0600-2571
Tetsuro Matsumoto http://orcid.org/0000-0003-2047-7028
Akihiko Masuda http://orcid.org/0000-0003-0572-0341
Yoshitomo Uwamino http://orcid.org/0000-0002-8359-3520
Stefan Roesler http://orcid.org/0000-0002-5920-0459
Markus Brugger http://orcid.org/0000-0002-3645-7091

References

[1] Tanaka S, Nakashima H, Sakamoto Y, et al. An experimental study on radiation streaming through a labyrinth in a proton accelerator facility of intermediate energy. Health Phys. 2001;81(4):406–418.

[2] Froeschl R. Radiation protection assessment of the proton irradiation facility and the CHARM facility in the east area. Tech Rep. 2014;1355933.

[3] Froeschl R, Brugger M, Roesler S. The CERN high energy accelerator mixed field (CHARM) facility in the CERN PS east experimental area. Proc Shielding Aspects Accel. 2014;3:14–25.

[4] Nakao N, Sanami T, Kajimoto T, et al. Roesler S and Infantino A. Attenuation length of high energy neutrons through a thick concrete shield measured by activation detectors at CHARM. J Nucl Sci Technol. 2020;57(9):1022–1034.

[5] Iliopoulou E, Bamidis P, Brugger M, et al. Measurements and FLUKA simulations of bismuth and aluminium activation at the CERN Shielding Benchmark Facility (CSBF). Nucl Instr Meth. 2018; A885:79–85.

[6] Kajimoto T, Sanami T, Nakao N, et al. Neutron energy spectrum measurement using an NE213 scintillator at CHARM. Nucl Instr Meth. 2018;B429:27–33.

[7] Kajimoto T, Sanami T, Nakao N, et al. Reproduction of neutron fluence by unfolding method with an NE213 scintillator. Nucl Instr Meth. 2018; A906:141–149.

[8] Nakao N, Uwamino Y, Tanaka K. Measurement of the neutron angular distribution from a beryllium target bombarded with a 345-MeV/u ^{238}U beam at the RIKEN RI beam factory. Nucl Instr Meth. 2018; B423:27–36.

[9] Gatignon L. Beam properties for the east area irradiation facility in the T8 beam line. Tech Rep. 2013;1270807.

[10] Bronson FL. Validation of the accuracy of the LabSOCS software for mathematical efficiency calibration of Ge detectors for typical laboratory samples. J Radioanal Nucl Chem. 2003;255:137–141.

[11] Sato T, Iwamoto Y, Hashimoto S, et al. Features of particle and heavy ion transport code system PHITS version 3.02. J Nucl Sci Technol. 2018;55:684–690.

[12] Furihata S. Statistical analysis of light fragment production from medium energy proton-induced reactions. Nucl Instrum Meth. 2000;B171:251–258.

[13] Boudard A, Cugnon J, David JC, et al. New potentialities of the Li'ege intranuclear cascade model for reactions induced by nucleons and light charged particles. Phys Rev. 2013;C87:014606.

[14] Nara Y, Otuka H, Ohnishi A, et al. Relativistic nuclear collisions at 10A GeV energies from p+Be to Au+Au with the hadronic cascade model. Phys Rev C. 2000;61(2):024901.

[15] Shibata K, Iwamoto O, Nakagawa T, et al. JENDL-4.0: a new library for nuclear science and engineering. J Nucl Sci Technol. 2011;48:1–30.

[16] Böhlen TT, Cerutti F, Chin MPW, et al. The FLUKA code: developments and challenges for high energy and medical applications. Nucl Data Sheets. 2014;120:211–214.

[17] Fassò A, Ferrari A, Ranft J, et al. FLUKA: a multiparticle transport code, Tech. Rep. CERN-2005-10, 2005, INFN/TC-05/11,SLAC-R-773.

[18] Maekawa F, Mollendorff UV, Wilson PPH, et al. Production of a dosimetry cross section set up to 50 MeV. Proc. 10th International Symposium on Reactor Dosimetry, 1999 Sep. 12–17, Osaka, Japan. Am Soc Test Mater. 2001;417.

[19] Kim E, Nakamura T, Uwamino Y, et al. Neutron activation cross section of ^{12}C, ^{27}Al, ^{59}Co, ^{nat}Cu and ^{209}Bi nuclides in the energy range 20 MeV to 200 MeV. Proc Int Conf Nucl Data Sci Technol. 1997;1503–1507.

[20] Froeschl R. A method for radiological characterization based on fluence conversion coefficients. J Phys Conf Ser. 2018;2018:10.

[21] Bozzato D, Froeschl R The Fluence Conversion Coefficients method: Applications to radiological characterization with the FLUKA and PHITS codes. 2020.